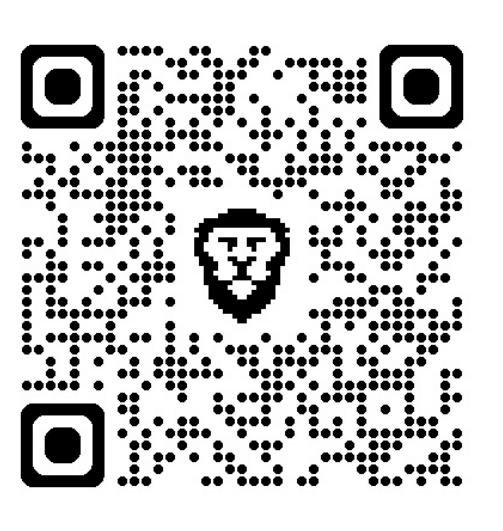


INDIVIDUALISED FIBRE-BALL WHITE MATTER IMAGING ANALYSIS OF DRUG RESISTANCE IN FOCAL EPILEPSY

COREY RATCLIFFE^{1,2}, LUKE ANDREWS^{1,3}, SHUBHABRATA BIWAS³, LEONARDO BONILHA⁴, ANTHONY MARSON^{1,3}, & SIMON S. KELLER^{1,3}

1. Department of Pharmacology and Therapeutics, Institute of Systems, Molecular & Integrative Biology, University of Liverpool, U.K.
 2. National Institute of Mental Health & Neuro Sciences (NIMHANS) Bangalore, India
 3. The Walton Centre NHS Foundation Trust, Liverpool, U.K.
 4. Department of Neurology, Medical University of South Carolina, Charleston, USA

Drug-resistant focal epilepsy is a network disorder, constituted by the agglomeration of distributed cortical abnormalities. White matter pathology is a common observation in drug-resistant epilepsy, but owing to the complexities of biophysical modelling, can be challenging to examine in vivo. This study uses a novel diffusion analysis pipeline to address limitations of white matter examinations whilst identifying potential white matter correlates of drug resistance in a focal epilepsy cohort.



INTRODUCTION

Drug resistance in focal epilepsy is the result of widespread network dysfunction. *In vivo* examination of the cerebral white matter is an invaluable aid to understanding the drug-resistant epilepsy network, but current Diffusion Weighted Imaging (DWI) methods have to overcome biophysical constraints to accurately represent underlying anatomy. Fixel-based Analysis (FBA; Fig. 1) is a DWI modelling approach that uses white matter constraints and intra-voxel fibre population modelling to address the issue of decomposing crossing fibre directions. Using a novel FBA pipeline and high-angular resolution DWI data, we aimed to characterise white matter abnormalities independent of some biophysical limitations.

METHODS

This study involved 15 healthy controls and 30 people with focal epilepsy (15 well-controlled, i.e. six-months of seizure freedom at the time of testing; 15 drug-resistant). All patients were recruited from, and diagnosed by epileptologists at, the Walton Centre NHS Foundation Trust. Fibre-ball (FBI) and Diffusion Kurtosis (DKI) imaging data were acquired at the (University of) Liverpool Magnetic Resonance Imaging Centre. Fixel maps were computed using a modified version of the recommended pipeline, first from the DKI data (bvals: 1000, 2000; bvecs: 30, 64), then the FBI data (bvals: 5000; bvecs: 128), and then from FBI-DKI data combined. FBA provides estimates of fibre density, fibre cross-section, and fibre density cross-section (FD, FC, and FDC, respectively), but scalar metrics can also be estimated from the same data.

First, the bilateral dDRTT tracts were estimated in all three sets of fixel maps, to evaluate their relative efficacy for accurate tractography. TractSeg was then used to segment the white matter template into tracts. From the DKI-FBI estimated fixel maps, whole brain comparisons of fixel and scalar metrics were computed between groups (with age and sex as covariates) using the permutation design in *fixelcfstats* and *mrcclusterstats* to correct for multiple comparisons - from significant voxels/fixels, local networks were seeded. Finally, tract-specific normative values for all metrics were computed from the controls, which were used to plot individual deviations from the norm.

RESULTS

The DKI-FBI fixel maps outperformed the others for estimating the left dDRTT (Fig. 2). Differences in FD and FDC between patient groups were found, and are presented in Fig. 5 alongside putative local networks seeded from significant fixels/voxels. Tracts that overlapped with regions of significant difference across any comparison were selected as tracts-of-interest for normative comparisons, which are also shown for fixel metrics of three individuals in Fig. 6.

CONCLUSIONS

As the angular resolution of the dataset increased, so too did the anatomical validity of tractography in a complex region; the superiority of our FBI-DKI dataset over traditional DKI approaches is therefore validated.

Fibre metric differences between the well-controlled and drug-resistant epilepsy participants suggest that the underlying pathology of drug-resistance is distinct from other epileptogenic network correlates, and implicates FD and FDC changes in the right cingulum and right middle longitudinal fascicle respectively. Conversely, well-controlled epilepsy appears to be related to the left isthmus and middle longitudinal fascicle. We also present individual differences in tract-specific metrics.

Figure 1 (Below, Left). An illustration of diffusion tensors and fixels. Whilst tensors represent the direction(s) of water movement within a 3D space (a volume element: voxel), fixels (fibre population within a voxel) represent a collection of pathways. This requires that certain assumptions about the biological properties of the tissue be made.

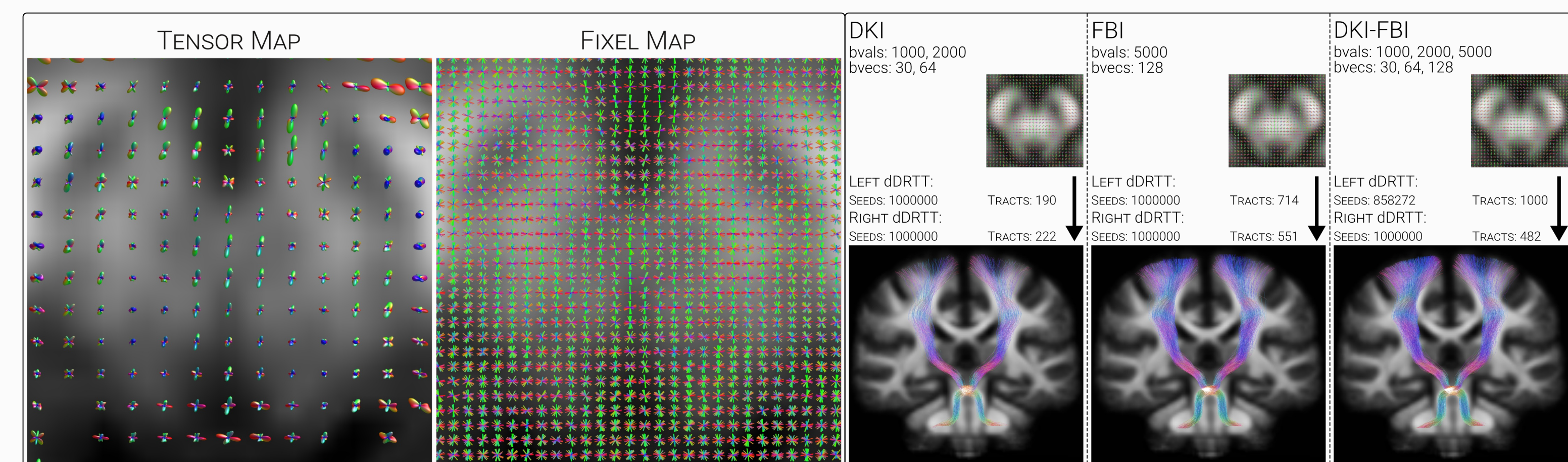


Figure 2 (Above, Right). Differences in streamline reconstruction when using different DWI datasets. The lower angular resolution of the DKI dataset makes it more difficult to resolve the crossing fibres in the brainstem, which both the FBI and the DKI-FBI dataset are more successful with. At a higher resolution, the bias towards attributing the crossed fibres to the left dDRTT becomes more pronounced, mirroring anatomy.

Figure 3 (Below, Top Left). a. Creation of the diffusion tensor. b. Putative representations of the underlying fibre anatomy by a tensor. c. Differences in kurtosis, underpinning DKI. d. Illustration of how crossing fibres may create uncertainty.

Figure 4 (Below, Bottom Left). Differences in angular resolution and shell number between different types of diffusion imaging scans.

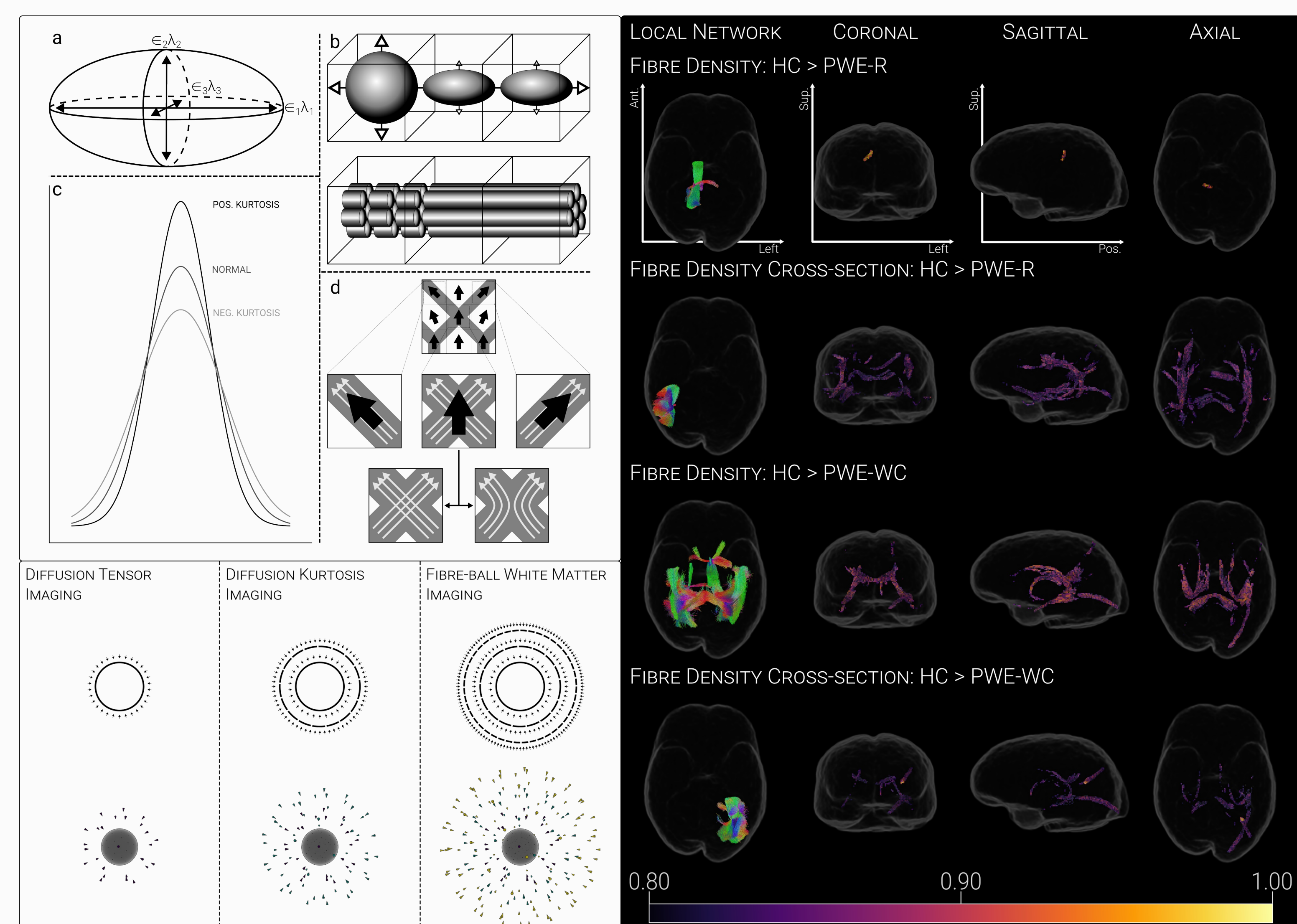


Figure 5 (Above, Right). Local networks and fixels identified as significantly different between different epilepsy phenotypes (i.e. well-controlled and drug-resistant) and controls, suggesting distinct underlying pathology. Networks were seeded only from fixels that were significant at the $p_{corr} < .050$ level, although fixels which exceeded the $p_{corr} < .200$ level are also presented for illustration.

Figure 6 (Below). Tract-specific differences in averaged fixel metrics between three example participants. FD, FDC, and logFC were averaged over TractSeg-defined tracts in each individual, transformed to normality using RNomi and standardised to averaged metrics computed from the 15 control participants. The grey line represents average, and the two dashed lines represent 2 standard deviations from average in both directions.

